J. Biochem. **127**, 1115–1120 (2000)

Conformational Changes of Dynein: Mapping and Sequence Analysis of ATP/Vanadate-Dependent Trypsin-Sensitive Sites on the Outer Arm Dynein β Heavy Chain from Sea Urchin Sperm Flagella[1]

Kazuo Inaba[2]

Asamushi Marine Biological Station, Graduate School of Science, Tohoku University, Asamushi, Aomori, Aomori 039-3501

Received January 21, 2000; accepted April 4, 2000

Conformational changes of dynein during ATP hydrolysis are demonstrated by the difference in the tryptic fragments of the dynein heavy chain between in the absence and presence of ATP and vanadate. Here tryptic sites in the presence of ATP and vanadate (Tav sites) have been mapped on the β heavy chain of outer arm dynein from sea urchin sperm flagella. Tav sites are located not only near the central catalytic domain which includes four P-loops, but also near the carboxyl-terminal coiled-coil region. The Tav2 site is located in the most carboxyl-terminal region, which is nearly 850 amino acid residues apart from the the fourth P-loop (P4 site). The region from the most amino-terminal Tav site (Tav1 site) to the Tav2 site covers approximately 2,100 amino acid residues, which is almost half the whole β heavy chain. Comparison of the sequences around the tryptic sites of the sea urchin β chain and those of the dynein heavy chains from other organisms reveals that the sequence around the Tav1 site is highly conserved in both cytoplasmic and axonemal dyneins but that around Tav2 sites is only conserved in axonemal dyneins, suggesting functional differences in the Tav2 region between the two subfamilies of dynein.

Key words: axoneme, dynein, flagella, molecular motor, sperm.

Dyneins are microtubule-dependent molecular motors involved in several microtubule-dependent intracellular translocation processes, including vesicle transport, nuclear segregation, and ciliary and flagellar motility. Dyneins are generally classified into cytoplasmic and axonemal ones, both of which are multisubunit complexes composed of two or three heavy chains and several intermediate and light chains (for reviews, see Refs. *1* and *2*).

The dynein heavy chains (~500 kDa) have an ATP-catalytic domain and are responsible for producing the force for microtubule movements (*3*, *4*). The four ATP-binding motifs, called P-loops, are located in the central one-third portion of the dynein heavy chain and are well-conserved among the dyneins from many organisms (*2*). The central catalytic domain along with an extending carboxyl-terminal region constitute the head portion of a dynein molecule (*5*). The amino-terminal one-third region constitutes the tail portion, which is thought to be important for the binding of other components, such as intermediate chains, several cargos or A-tubules of doublet microtubules (*1*). The portion between the central and carboxyl-terminal regions forms a coiled-coil domain which constitutes a stalk extending from each head and is suggested to be responsible for ATP-sensitive microtubule-binding (*6*).

Although the cytoplasmic dynein is a homodimer of a single species of heavy chain, the axonemal dynein is composed of heterogenous dynein heavy chains which are encoded by separate genes and have distinct functions in axonemal motility (*7*, *8*). In *Chlamydomonas*, *Tetrahymena*, or *Paramecium*, the outer arm dynein contains three heavy chains, termed α, β, and γ. The outer arm dyneins from most multicellular organisms contain a heterodimer of heavy chains (*9*), for example, the outer arm dynein from sea urchin sperm flagella contains α and β heavy chains (*10*). In the outer arm dynein from sea urchin sperm flagella, it is conceivable that the β heavy chain functions in force generation, and the α heavy chain mediates structural and rigor binding of β-containing subparticles to microtubules (*11*, *12*).

The sliding of microtubules is caused by mechanochemical transduction by dynein. The rigor state of dynein dissociates from microtubules by binding ATP, followed by ATP hydrolysis into ADP and P_i. The release of these products is the rate-limiting step and is presumed to be responsible for force production (*13*, *14*). Vanadate (V_i) acts as an analogue of inorganic phosphate (P_i) and can form a stable dynein-ADP-V_i complex which mimics the relaxed state. The morphology of the rigor and relaxed states of dynein in an axoneme apparently differs *in situ* (*15–17*), although the molecular nature of this conformational change is poorly understood.

Among several tools for studying protein conformations, limited proteolytic digestion has been useful for surveying the conformation of the dynein molecule (*18–22*). We have

[1]This work was carried out in part under the NIBB Cooperative Research Program (99–136), and supported by Grants-in-Aid from the Ministry of Education, Science, Sports and Culture of Japan, and by a grant from Narishige Zoological Science Award.
[2]For correspondence: Tel: +81-177-52-3394, Fax:+81-177-52-2765, E-mail: inaba@biology.tohoku.ac.jp

detected a conformational change of the outer arm dynein from sea urchin sperm flagella by means of tryptic digestion, and revealed that dynamic conformational changes occur in the dynein β heavy chain between the rigor and relaxed states (*18*). The conformational changes of the β heavy chain also involve changes in the interactions with the α heavy chain (*20*) and the intermediate chain 1 (*23*, *24*). The mapping of Tav sites, which become susceptible to trypsin in the presence of ATP/V_i, has been performed previously for the sea urchin β heavy chain by means of a biochemical procedure (*21*). However, since the primary structure of the β heavy chain is now available (*25*, *26*), it is possible to map the sites much more precisely. Here these sites are determined by analyzing the amino-terminal amino acid sequences of tryptic fragments of the β heavy chain and the sequences or secondary structure around these sites are investigated.

MATERIALS AND METHODS

Isolation of Dynein—The flagellar axoneme was prepared as described previously (*27*). The outer arm dynein was isolated from the axoneme by extraction with a high salt solution, followed by 5–20% sucrose density gradient centrifugation (*18*). The dynein was dialyzed against a buffer containing 0.15 M KCl, 2 mM $MgCl_2$, 1 mM EGTA, 10 mM Tris-HCl, pH 8.0, and 0.1 mM DTT, to remove sucrose.

Tryptic Digestion and Peptide Sequencing of Tryptic Fragments—The outer arm dynein (~0.5 mg/ml) was digested with TPCK-treated trypsin (Sigma, 300 μg/ml) at 20°C for 30 min. The reactions were terminated by the addition of soybean trypsin inhibitor to 2 mg/ml. The tryptic fragments were separated by SDS–polyacrylamide gel electrophoresis (*28*) with a 5% polyacrylamide gel as the separating gel. The proteins were electrophoretically transferred to a PVDF membrane (Applied Biosystems, Pro-Blott™), and stained with Coomassie Brilliant Blue R-250, and then the amino-terminal sequence was determined with a Applied Biosystems Model 476 protein sequencer.

Sequence Analysis—The similarities of the sequence around each tryptic site between the sea urchin dynein β heavy chain and other dynein heavy chains were examined with the GCG program BESTFIT with default parameters. Overall comparison between the sea urchin β and *Chlamydomonas* β heavy chains was performed with the GCG program COMPARE. The coiled-coil region in the sea urchin β heavy chain was predicted using the Lupas algorithm COILS (*29*). Multiple alignment was performed with CLUSTALW.

RESULTS

Proteolytic Pathway of the β Heavy Chain—The tryptic fragments of outer arm dynein from sea urchin sperm flagella in the absence and presence of ATP/V_i are shown in Fig. 1. All the fragments observed are derived from the β heavy chain (*19*). The difference in the fragments produced in the absence and presence of ATP/V_i is considered to be due to the difference in the conformation of the β heavy chain between the two conditions (*18*). The digestion pathway of the β heavy chain was previously determined by means of V_i-dependent photocleavage and antibodies which recognize a specific region of the β heavy chain (*21*). In the absence of ATP/V_i, two products, 165 and 135 kDa fragments, are produced by trypsin through cleavage at the T1, T2, and Ts sites. In the presence of ATP/V_i, the T2 site becomes less susceptible to trypsin, resulting in the production of a relatively stable 300 kDa fragment, and four new sites, named the Tav1–Tav4 sites, become more susceptible to trypsin to produce 200, 150/148, 105, and 96 kDa fragments (Fig. 2).

Mapping of Tryptic Sites on the β Heavy Chain—To localize the tryptic sites more precisely, each fragment separated by SDS-PAGE was transferred to a PVDF membrane and then subjected to amino-terminal amino acid sequencing (Table I). The sequences were searched for in the complete amino acid sequence of the outer arm dynein β heavy chain from sea urchin (*25*; Accession number D01021). Although some amino acids could not be identified, the sequences completely matched the following portions of the β heavy chain; N2512 to I2525 for the amino-terminal sequence of the 200 kDa fragment, F1379 to L1393 for the 165 kDa fragment, A1571 to F1586 for 150 kDa, L1572 to P1584 for 148 kDa, T3324 to N3339 for 135 kDa, A1571 to Y1587 for 105 kDa, and I3648 to A3660 for 96 kDa. Thus all the tryptic sites except the Tav3 site were

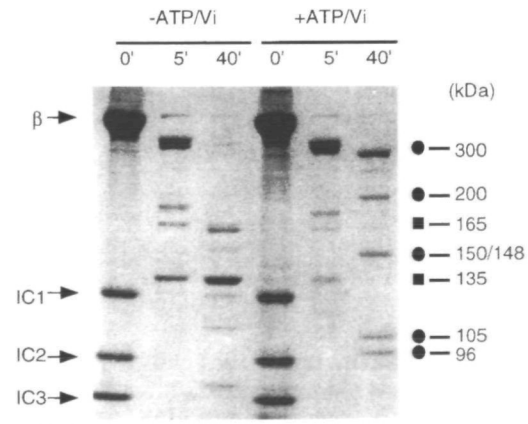

Fig. 1. **SDS-PAGE showing the difference in the tryptic fragments of outer arm dynein between in the absence or presence of ATP/V_i.** Outer arm dynein was digested with trypsin at 20°C for 5 and 40 min. Major tryptic fragments are indicated by closed circles (in the presence of ATP/V_i) and closed squares (in the absence of ATP/V_i) with the molecular masses given in kDa.

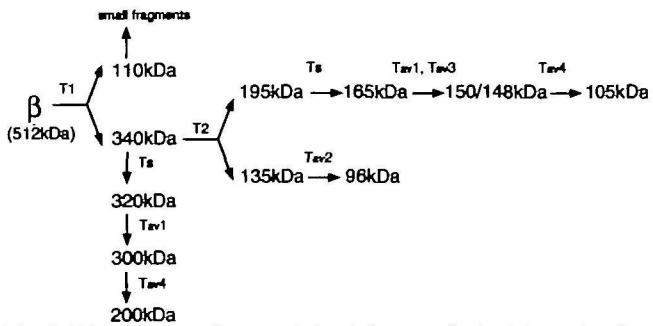

Fig. 2. **Digestion pathway of the β heavy chain.** The molecular size of each tryptic fragment is indicated in kDa. The T1 and T2 sites are primary sites for the production of 195 and 135 kDa fragments. The 110 kDa fragment is further degraded into fragments. The Ts site is the tryptic site which is cleaved in the presence of salt and Mg^{2+} (*21*). Tav sites are cleaved by trypsin in the presence of ATP/V_i.

determined and mapped on the β heavy chain (Fig. 3).

The Tav1 and Tav4 sites are located relatively near the P1 and P3-loop, respectively. The Tav2 site is located at more than 300 amino acids carboxyl-terminal from the T2 site and nearly 850 amino acids apart from the P4 site. The

TABLE I. **Amino-terminal amino acid sequences of tryptic fragments.**

Fragment	Sequence
200K	NYGPPGTKKLVYFI
165K	FTMDKEXTLXDLLAL
150K	ALAEYLETKRLAFPRF
148K	XLAEYLEXKRLAFP
135K	TITLANRLVGGLASEN
105K	ALAEYLETKRLAFPRFY
96K	INEARELYRPAAA

X: undefined amino acid.

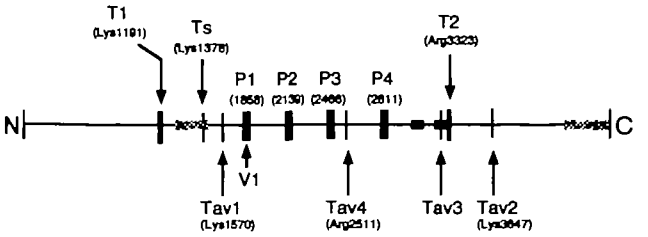

Fig. 3. **Mapping of tryptic sites on the β heavy chain.** The number at each P-loop shows the lysine residue in the ATP-binding consensus sequence. The V1 site is the vanadate-mediated photocleavage site (*30*). The dark shaded area shows the coiled-coil region, which forms a B-link stalk structure (*6*) (residues 3028–3083 and 3262–3303). The light shaded area shows the homologous region whose deletion causes both loss of photocleavage and ATP-insensitive rigor binding to microtubules in rat cytoplasmic dynein (residues 1252–1413 and 4103–4463) (*6*).

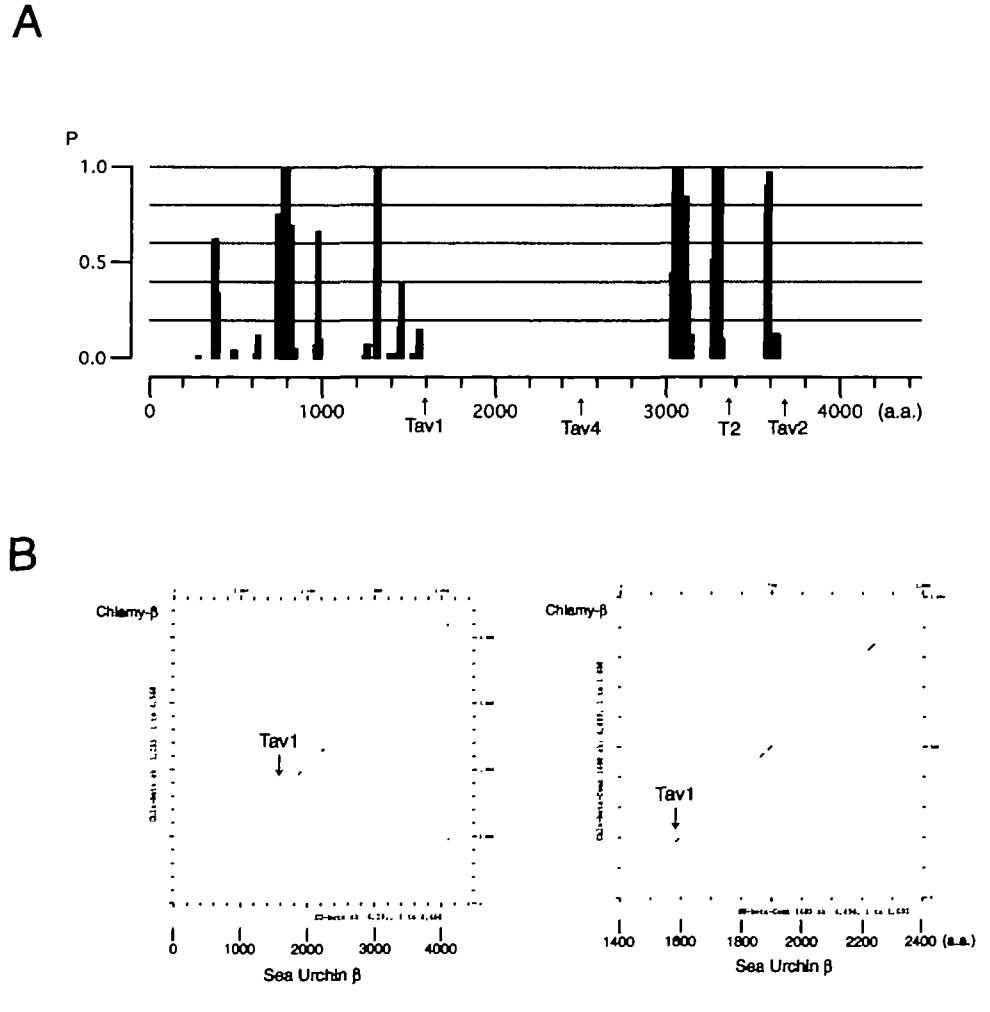

Fig. 4. **The structure of the sea urchin β heavy chain and comparison with *Chlamydomonas* outer arm dynein heavy chains.** A: Prediction of coiled-coil regions in the sea urchin β heavy chain with the Lupas algorithm (*29*), with a window length of 28 on the MTIDK matrix. Probability (P) against amino acid residues (a.a.) is shown. B: Pairwise sequence comparison between whole (left) and central regions (right) of the sea urchin β and *Chlamydomonas* β dynein heavy chains, performed with the GCG program COMPARE with a compare window of 30 and a stringency of 135. C: Multiple alignment of highly conservative region near the Tav1 site among the sea urchin β (upper; residues 1565–1604), *Chlamydomonas* β (middle; residues 1632–1671), and α (lower; 1432–1471) heavy chains. The alignment was performed with CLUSTAL W. Asterisks, colons and dots indicate identical residues in all sequences in the alignment, conserved substitutions and semi-conserved substitutions, respectively.

TABLE II. **Pairwise % similarity comparisons of the region around tryptic sites.**

	SU-β				
	P1-P4	Tav1	Tav4	T2	Tav2
SU-α	49	NA	**58**	NA	NA
Chla-α	62	**67**	**70**	47	**63**
Chla-β	62	**70**	**66**	44	**65**
Chla-γ	50	(55)	**54**	48	**61**
Chla-IA	54	**59**	**59**	41	49
Tetra-β	60	57	**61**	45	**60**
Parame-β	60	**61**	**63**	44	56
SU-cyto	46	**53**	(70)	NA	NA
Parame-cyto	48	**54**	(60)	39	38
Dicty-cyto	46	**55**	(65)	32	42
Droso-cyto	46	**53**	(70)	30	43
Rat-cyto	47	**53**	(70)	33	45
	Parame-cyto				
	P1-P4	Tav1	Tav4	T2	Tav2
SU-cyto	70	**73**	(90)	NA	NA
Dicty-cyto	70	**80**	(90)	56	52
Droso-cyto	69	**73**	(85)	61	52
Rat-cyto	70	**71**	(90)	61	53

The regions of each dynein heavy chain homologous to the central catalytic (P1-P4; residues 1852–2811), Tav1 (residues 1540–1600), Tav4 (residues 2481–2541), T2 (residues 3293–3353), and Tav2 (residues 3617–3677) regions of the sea urchin β heavy chain were searched with BLAST and then compared with the GCG program BESTFIT. The lower part of the table shows comparison of cytoplasmic dyneins against the *Paramecium* cytoplasmic dynein heavy chain. The % similarity, which is the same or higher than that in the P1–P4 region in each pair, is indicated in boldface. The pair for which the sequence of the homologous region is not available in the database is denoted by NA. The value in parentheses show % similarity limited to the short homologous region hit by BESTFIT (29 residues for the Tav1 region for SU-β *vs.* Chla-γ; 22–25 residues for SU-β *vs.* cytoplasmic dyneins, or Parame-cyto *vs.* cytoplasmic dyneins. See the text). The dynein heavy chains and the accession numbers in the database are sea urchin outer arm dynein β (SU-β; D01021) and α (SU-α; U03970) heavy chains; *Chlamydomonas* outer arm dynein α (Chla-α; L26049), β (Chla-β; U02963), and γ (Chla-γ, Q39575) heavy chains; *Chlamydomonas* inner arm dynein heavy chain 1 (dhc 1)(Chla-IA; AJ243806); *Tetrahymena* outer arm dynein β heavy chain (Tetra-β; AF072878); *Paramecium* outer arm dynein β heavy chain (Parame-β; Y19464); sea urchin cytoplasmic dynein heavy chain (SU-cyto; Z21941); *Paramecium* cytoplasmic dynein heavy chain (Parame-cyto; U20449); *Dictyostelium* cytoplasmic dynein heavy chain (Dicty-cyto; Z15124); *Drosophila* cytoplasmic dynein heavy chain (Droso-cyto; L23195); and rat cytoplasmic dynein heavy chain (rat-cyto; L08505).

region from the Tav1 site to the Tav2 site covers approximately 2,100 amino acids. This is almost half the whole β heavy chain.

In this study, the Tav2 site was mapped at a position different from that previously reported (*21*). Since the Tav2 site was previously determined using carboxypeptidase digestion, followed by peptide mapping, this was probably due to unexpected cleavage by an endopeptidase contaminating the carboxypeptidase. The Tav3 site has not been determined in the present study, but it should be ~2 kDa amino-terminal from the T2 site, as described previously (*21*).

Correlation of Tryptic Sites to the Secondary Structure of the β Heavy Chain—The coiled-coil regions were predicted and correlated with the tryptic sites. The result showed that the Tav1, T2, and Tav2 sites are all located at the carboxyl-ends of the coiled-coil region (Fig. 4A). Although the β heavy chain has no long α-helix coiled-coil structure in the amino-terminal region like myosin or kinesin (*25*), analysis of the coiled-coil region by mean of the Lupas algorithm (*29*) has shown that there are many short coiled-coil regions in the amino-terminal region of the β heavy chain. The Tav1 site is located at the carboxyl-end of this cluster of short coiled-coil regions (Fig. 4A).

On the other hand, a previous study has shown that the coiled-coil region between the central catalytic and carboxyl-terminal domains at residues 3,028–3,083 and 3,262–3,303 appears to form a stalk structure responsible for ATP-sensitive microtubule binding (*6*). In the present study, another coiled-coil portion has been found in this region at around residue 3,600 with the Lupas algorithm (Fig. 4A). The T2 and Tav2 sites are located at the carboxyl end of the second and third coiled-coil regions, respectively (Fig. 4A).

Sequence Comparison between the Sea Urchin β and Chlamydomonas β Heavy Chains—Analysis of homologous regions between the sea urchin β and *Chlamydomonas* β heavy chains revealed that the Tav1 site is located within the very conservative region between the two species (Fig. 4B). When the analysis was performed with the GCG program COMPARE at high stringency, highly conservative regions (HCRs) between two heavy chains could be visualized (Fig. 4B). The most amino-terminal HCR is around the Tav1 site, and the 40 amino acids around the Tav1 the site, (residues 1565–1604) of the sea urchin β chain show 83 and 78% identity with the corresponding region of the *Chlamydomonas* β and α heavy chains, respectively (Fig. 4C). There are two other HCRs in the central portion and one HCR in the carboxyl-terminal portion (Fig. 4B, left).

Sequence Comparisons around Tryptic Sites among Several Dynein Heavy Chains—Because tryptic sites are considered to be located between structural domains in the dynein heavy chain, they must have important roles in the dynein function. Hence, in this study, sequences around each tryptic site are compared among several dynein species (Table II). The result showed that the sequences around some tryptic sites are surprisingly conserved among several dyneins.

First, the Tav1 region shows high similarity with those of axonemal dyneins, including inner arm dynein, and cytoplasmic dyneins, except that the *Chlamydomonas* γ heavy chain has only a 29 amino acid region homologous to the Tav1 region of the sea urchin β heavy chain.

Second, the Tav4 region is also conserved among axonemal and cytoplasmic dyneins, although the conservation is limited to a short region (20–25 amino acid residues) in the case of cytoplasmic dyneins. The similarity of the sea urchin β heavy chain to *Chlamydomonas* β is much higher in the Tav1 region than that in the Tav4 region, but the similarity to *Chlamydomonas* α, *Tetrahymena* β, or *Paramecium* β in the Tav4 region is higher than that in the Tav1 region. The homologous regions detected with the BESTFIT program around the Tav1 site between the sea urchin β and cytoplasmic dynein heavy chains range from 50 to 60 amino acid residues, whereas those around the Tav4 region only range up to 25 amino acid residues. However, they show high similarity to the sea urchin β heavy chain in this short region (Table II, parentheses). This region also shows very high homology among cytoplasmic dyneins.

Third, in contrast to the Tav1 or Tav4 site in the central catalytic region, the carboxy terminal T2 region shows no significant similarity among the dynein heavy chains. The Tav2 region, however, shows high similarity between the sea urchin β and axonemal dyneins, especially the *Chlamydomonas* α, β, or γ heavy chain, although it shows low similarity between the sea urchin β and cytoplasmic dynein heavy chains (Table II).

DISCUSSION

In this study, four tryptic sites whose susceptibilities to trypsin change in the presence of ATP/Vi were mapped on the β heavy chain of sea urchin outer arm dynein. Tav sites are located not only in the central catalytic domain but also near the carboxyl-terminal coiled-coil region, and the region from the Tav1 site to the Tav2 site covers approximately 2,100 amino acid residues, this length being almost half that of the β heavy chain.

The predicted secondary structure suggests that the β heavy chain is composed of an amino-terminal α-helix dominant region, a central β sheet dominant region containing four P-loops, and a carboxyl-terminal β sheet dominant region (see Ref. *25*). Both the β sheet dominant domains are split by three to four short α-helix dominant regions. When the conformation-dependent tryptic sites (Fig. 3) were collated with the predicted secondary structure, all the sites could be located at the boundary between the α-helix dominant and β-structure dominant regions.

The Tav1 and Tav4 sites located in the central catalytic domain are well conserved in both cytoplasmic and axonemal dyneins, suggesting that these site are closely related to the fundamental process of the dynein mechanochemical cycle, such as ATP hydrolysis. The Tav1 site is located at ~90 amino acid residues toward the amino-terminus from the P1 site, which is believed to be the primary ATP hydrolytic site (*25*, *26*, *30*). This appears to be related to the fact that deletion of the region near the Tav1 site causes the loss of the photocleavage of the dynein heavy chain and ATP-insensitive rigor binding to microtubules (*6*). The prediction of coiled-coil regions shows that the Tav1 site is located at the end of a long cluster of short potential coiled-coils in the amino-terminal region (Fig. 4A). This is reminiscent of the 20 kDa region of myosin subfragment 1, which is located at the neck of the globular head and is connected to a long coiled-coil tail region (*31*). This is interesting in the light of the recent finding suggesting that this region of myosin swings during the power stroke (*32*, *33*).

The T2 site, which becomes less sensitive to trypsin in the presence of ATP/V_i (*19*), is located at 500 amino acid residues toward the carboxyl-terminus from the P4 site. The region around the T2 site forms a coiled-coil structure (Figs. 3 and 4A), which is observed on electron microscopy as the "stalk" (*15*) and is involved in microtubule binding (*6*). This region also appears to be involved in the coordination of dynein arm activity, since the deletion around this region, known as the *sup-pf1* mutation in *Chlamydomonas*, modifies the activity of outer arm dynein and restores motility to paralyzed central pair/radial spoke defective mutants (*34*). Although the region around the T2 site is less conserved among several dynein heavy chains, the secondary structures are well conserved among cytoplasmic and axonemal dyneins (*6*). The T2 site is located at the carboxyl-terminal end of the α-helical coiled-coil region (Fig. 4A). The low sensitivity to trypsin around this region in the dynein-ADP-V_i complex may be related to the displacement of this region during the power stroke (*17*).

The Tav2 site is located far from central catalytic P-loops: It is 324 residues apart from the T2 site and 836 residues apart from the P4 site toward the carboxyl-terminus. However, it becomes susceptible to trypsin in the dynein-ADP-V_i complex, suggesting that the conformational change around the Tav2 site is closely coupled to ATP hydrolysis by the central catalytic domain. The 165 kDa tryptic fragment derived from the central catalytic domain and the 135 kDa carboxyl-terminal fragment are strongly associated with each other (*18*). Hence, there would be a mechanism which induces the conformational changes of the non-catalytic carboxyl-terminal domain through intramolecular interaction between the two regions. This idea is supported by the fact that deletion of the carboxyl-terminal region causes the loss of photocleavage and rigor-like interaction with microtubules (*6*), and that there are two HCRs near the carboxyl-terminus (Fig. 4B). Interestingly, the region around the Tav2 site is conserved in the heavy chain of outer arm dynein but not in either the inner arm or cytoplasmic dynein (Table II), suggesting a certain role of this region in the function of outer arm dynein.

Overall sequence comparison among the outer arm dynein heavy chains of sea urchin and *Chlamydomonas* indicates that the sea urchin α heavy chain is homologous to the *Chlamydomonas* γ heavy chain (*4*). These two heavy chains appear to have separated rapidly from the branch carrying the sea urchin β or *Chlamydomonas* α and β heavy chains, as shown on phylogenetic tree analysis (*4*). Comparison around the Tav site also supports this idea (Table II). As for the property of translocation of microtubules, however, the *Chlamydomonas* γ heavy chain translocates microtubules whereas the sea urchin α heavy chain does not, although both heavy chains are bound to microtubules in both ATP-sensitive and -insensitive manners (*11*, *12*, *35*). In terms of force production for microtubule translocation, as discussed above, it is interesting to compare the sequences of the Tav1 and Tav2 regions between the sea urchin α and *Chlamydomonas* γ heavy chains. The molecular cloning of the full length sea urchin α heavy chain will provide more information on this issue.

In summary, the present study clearly shows that the dynein β heavy chain undergoes not local but global conformational changes during ATP hydrolysis, which has also been shown in morphological studies using electron microscopy (*15–17*). The conformational changes of the dynein heavy chain involve the regions around the boundaries between the α-helix region and the β-sheet structure, and are characterized by the involvement of the long carboxyl-terminal region, which would be related to the displacement of the dynein head (*17*) and to the variable angulation of the B-link or stalk (*15*, *17*). These changes must be caused by intracellular transmission of some structural signal from the central catalytic domain to the carboxyl-terminal domain, resulting in the application of tension on the stalk, which is responsible for exerting the force.

The protein sequencing was conducted at the Misaki Marine Biological Station, The University of Tokyo, when the author was a member there. The author wishes to thank the staff of the Misaki

Marine Biological Station, and Fukaura Fisherman's Associations for providing the sea urchins.

REFERENCES

1. Holzbaur, E.L.F. and Vallee, R.B. (1994) Dyneins: molecular structure and cellular function. *Ann. Rev. Cell Biol.* **10**, 339–372
2. Milisav, I. (1998) Dyneins and dynein-related genes. *Cell Motil. Cytoskeleton.* **39**, 262–272
3. Ogawa, K. and Mohri, H. (1996) A dynein motor superfamily. *Cell Struct. Funct.* **21**, 343–349
4. Gibbons, I.R. (1996) The role of dynein in microtubule-based motility. *Cell Struct. Funct.* **21**, 331–342
5. Ogawa, K. (1992) Primary structure and function of a dynein motor molecule. *Zool. Sci.* **9**, 265–274
6. Gee, M.A., Heuser, J.E., and Vallee, R.B. (1997) An extended microtubule-binding structure within the dynein motor domain. *Nature* **390**, 636–639
7. Asai, D.J. (1995) Multi-dynein hypothesis. *Cell Motil. Cytoskeleton.* **32**, 129–132
8. Gibbons, I.R. (1995) Dynein family of motor proteins: present status and future questions. *Cell Motil. Cytoskeleton.* **32**, 136–144
9. Mohri, H., Inaba, K., Kubo-Irie, M., Takai, H., and Yano-Toyoshima, Y. (1999) Characterization of outer arm dynein in β sea anemone, *Anthopleura midori*. *Cell Motil. Cytoskeleton* **44**, 202–208
10. Bell, C.W. and Gibbons, I.R. (1982) Structure of dynein 1 outer arm in sea urchin sperm flagella. II. Analysis by proteolytic cleavage. *J. Biol. Chem.* **257**, 516–522
11. Moss, A.G., Gatti, J.L., and Witman, G.B. (1992) The motile β/IC1 subunit of sea urchin sperm outer arm dynein does not form a rigor bond. *J. Cell Biol.* **118**, 1177–1188
12. Moss, A.G., Sale, W.S., Fox, L.A., and Witman, G.B. (1992) The α subunit of sea urchin sperm outer arm dynein mediates structural and rigor binding to microtubules. *J. Cell Biol.* **118**, 1189–1200
13. Omoto, C.K. and Johonson, K.A. (1986) Activation of the dynein adenosine triphosphatase by microtubules. *Biochemistry* **25**, 419–427
14. Tani, T. and Kamimura, S. (1998) Reactivation of sea urchin sperm flagella induced by rapid photolysis of caged ATP. *J. Exp. Biol.* **201**, 1493–1503
15. Goodenough, U.W. and Heuser, J.E. (1982) Substructure of the outer arm dynein. *J. Cell Biol.* **95**, 798–815
16. Tsukita, Sh., Tsukita, S., Usukura, J., and Ishikawa, H. (1983) ATP-dependent structural changes of the outer arm dynein arm in *Tetrahymena* cilia: a freeze-etch replica study. *J. Cell Biol.* **96**, 1480–1485
17. Burgess, S.A. (1995) Rigor and relaxed outer dynein arms in replicas of cryofixed motile flagella. *J. Mol. Biol.* **250**, 52–63
18. Inaba, K. and Mohri, H. (1989) Dynamic conformational changes of 21S dynein ATPase coupled with ATP hydrolysis revealed by proteolytic digestion. *J. Biol. Chem.* **264**, 8384–8388
19. Inaba, K. and Mohri, H. (1989) Two states of the conformation of 21S outer arm dynein coupled with ATP hydrolysis. *J. Biochem.* **106**, 249–354
20. Inaba, K., Ono, M., and Mohri, H. (1990) Conformational changes of the β chain of the outer-arm dynein from sea urchin sperm flagella coupled with ATP hydrolysis. *J. Biochem.* **108**, 663–668
21. Inaba, K., Ogawa, K., and Mohri, H. (1991) Mapping of ATP-dependent trypsin-sensitive sites on the β chain of outer-arm dynein from sea urchin sperm flagella. *J. Biochem.* **110**, 795–801
22. Mocz, G., Farias, J., and Gibbons, I.R. (1991) Proteolytic analysis of domain structure in the β heavy chain from sea urchin sperm flagella. *Biochemistry* **30**, 7225–7231
23. Inaba, K. (1994) Cross-linking of β heavy chain subunit of dynein from sea urchin sperm flagella by dimethyl suberimidate. *Biomed. Res.* **15**, 123–126
24. Inaba, K. (1995) ATP-dependent conformational changes of dynein: Evidence for changes in the interaction of dynein heavy chain with the intermediate chain. *J. Biochem.* **117**, 903–907
25. Ogawa, K. (1991) Four ATP-binding sites in the midregion of the β heavy chain of dynein. *Nature* **352**, 643–645
26. Gibbons, I.R., Gibbons, B.H., Mocz, G., and Asai, D.J. (1991) Multiple nucleotide-binding sites in the sequence of dynein β heavy chain. *Nature* **352**, 640–643
27. Inaba, K., Mohri, T., and Mohri, H. (1988) B-band protein in sea urchin sperm flagella. *Cell Motil. Cytoskeleton* **10**, 506–517
28. Laemmli, U.K. (1970) Cleavage of structural proteins during the assembly of the head of bacteriophage T4. *Nature* **227**, 680–683
29. Lupas, A. (1996) Prediction and analysis of coiled-coil structures. *Methods Enzymol.* **266**, 513–525
30. Gibbons, I.R., Lee-Eiford, A., Mocz, G., Phillipson, C.A., Tang, W.-J.Y., and Gibbons, B.H. (1987) Photosensitized cleavage of dynein heavy chains: cleavage at the "V1" site by irradiation at 365 nm in the presence of ATP and vanadate. *J. Biol. Chem.* **262**, 2780–2786
31. Gulick, A.M. and Rayment, I. (1997) Structural studies on myosin II: communication between distant protein domains. *BioEssays* **19**, 561–569
32. Suzuki, Y., Yasunaga, T., Ohkura, R., Wakabayashi, T., and Sutoh, K. (1998) Swing of the lever arm of a myosin motor at the isomerization and phosphate-release steps. *Nature* **396**, 380–383
33. Dobbie, I., Linari, M., Piazzesi, G., Reconditi, M., Koubassova, N., Ferenczi, M.A., Lombardi, V., and Irving, M. (1998) Elastic bending and active tilting of myosin heads during muscle contraction. *Nature* **396**, 383–387
34. Porter, M.E., Knott, J.A., Gardner, L.C., Mitchell, D.R., and Dutcher, S.K. (1994) Mutations in the *SUP-PF-1* locus of *Chlamysomonas reinhardtii* identify a regulatory domain in the β-dynein heavy chain. *J. Cell Biol.* **126**, 1495–1507
35. Sakakibara, H. and Nakayama, H. (1998) Translocation of microtubules caused by the αβ, β and γ outer arm dynein subparticles of *Chlamydomonas*. *J. Cell Sci.* **111**, 1155–1164